Transient multiwave mixing in a nonlinear medium

I. C. Khoo and Ping Zhou
Department of Electrical Engineering, The Pennsylvania State University, University Park, Pennsylvania 16802
(Received 24 July 1989)

We present a detailed quantitative theory of transient multiwave mixing effects in a nonlinear medium produced by two incident coherent laser beams. Our theory accounts for all the relevant parameters such as laser pulse widths, medium response times, nonlinearities, interaction length, intensities, beam ratio, phase-modulation effects, losses, side diffractions, and explicitly shows how the dynamics and the multiwave mixing processes are interrelated with these parameters. The crucial role played by the diffracted beams and the time-dependent phase shifts among the beams and the interplay among the various intensity and index gratings are explicitly evaluated. In particular, the gain experienced by a weak incident probe beam via these mixing effects from the incident strong pump beam is investigated as a function of the aforementioned parameters.

I. INTRODUCTION

The study of optical wave mixing dates back to the early years of nonlinear optics.[1-3] Theories and experiments dealing with some of these processes, such as second- and third-harmonic generations, stimulated scatterings, two- and four-wave mixing, etc., have by now been standardized for many years. Recently, with the emergence of highly nonlinear materials, many of these so-called standardized effects have been found to assume several new, interesting, and potentially very useful forms.[4-8]

In particular, studies of stationary multiwave mixing effects involving an incident pump and a probe beam (c.f. Fig. 1) have led to new theoretical understandings and experimental results on beam amplification,[4-7] phase conjugation, and self-oscillation processes.[8] The fundamental process of amplifying a weak beam by a strong beam of the same frequency by wave mixing in a nonlinear medium can be mediated, in the stationary case, either by a naturally present phase shift (in photorefractive materials[9]) between the refractive and laser intensity gratings, or, in nonphotorefractive media (e.g., Kerr media, thermal index media), by the diffracted beams which are generated from scattering of the incident waves from the index grating (produced by the two incident waves). The former process is termed two-wave mixing (as it involves only the pump and the probe beams), and the latter process is generally called multiwave mixing effect [as they involve other (diffracted) beams besides the pump and the probe].

In the stationary case, as a result of the diffusive nature of the underlying optical nonlinearities (e.g., collective reorientations and thermal effects in liquid crystals, electronic diffusion in semiconductor etc.), the wave-mixing effects diminish rapidly while increasing the angle of intersection between the incident laser beams (i.e., decreasing the refractive index grating constant induced by these lasers). The phase-matching requirement for producing the side diffraction also requires that the medium be thin and/or the wave mixing angle be small. Although this limitation (of having to use a very small angle) can be largely offset if the laser is in the infrared regime (e.g., 10.6-μm CO_2 laser), it presents, in general, a serious handicap for applications using cw visible or near infrared laser.

In this paper, we present a detailed theoretical discussion that emphasizes the transient aspects of these wave mixing effects for the case where incident laser pulse widths are shorter or comparable to the medium response time. Our theory is an extension of the formalism employed by Vinetskii *et al.*[10] The new features of our theory include (i) quantitative and explicit formulation of the intensity and phase equations involving the two incident beams and two side diffracted beams. This four-beam approach is fundamentally a more self-consistent treatment in that it allows one to study the dependence of the wave mixing process on the relative intensity ratio of the pump to the probe beam. This ratio dependence is important if one envisions using these *multiwave mixing effects* to construct a ring oscillator,[11] for example, starting with a "probe" beam that originates as scattered noise from the pump beam. As the probe beam intensity increases, the pump to probe beam ratio will decrease and

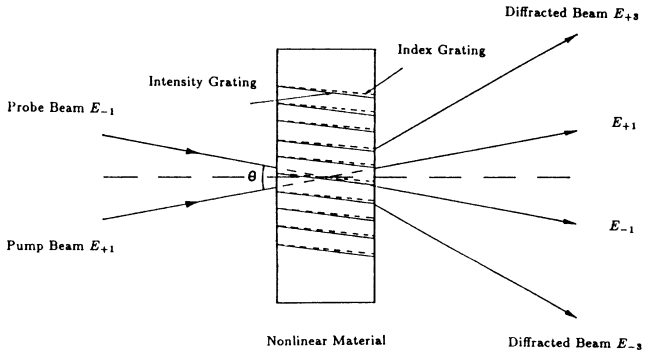

FIG. 1. Schematic of the transient multiwave mixing involving a pump, a probe, and two side diffracted beams.

thus will affect the wave mixing gain. Similar types of wave-mixing devices, e.g., phase conjugator, also depend critically on this beam ratio.[7] Another new feature is (ii) explicit evaluation of the probe-beam gain for the large gain regime (i.e., gain $\gg 1$) as a function of time, beam ratio, wave mixing angles, intensities, etc. This information is not available by approximate or perturbative solutions of the problem, but they are crucial for examining the limits or optimization of the probe-beam gain effect. Also included are (iii) explicit solution and illustrations of the various phases and phase shifts involved in the multiwave couplings that affect the transient multiwave energy-exchange process. In particular, we point out how the intensity-dependent phase-modulation effect could dominate over the phase mismatch experienced by the diffracted beams, resulting in their nonvanishing (in fact, substantial) contribution to the wave mixing effect under geometrical conditions where they normally would be of vanishing amplitude.

In Sec. II, we present the basic theoretical formulation, followed by some discussion of the pertinent features of transient multiwave mixing effect. In Sec. IV, the equations and various experimentally accessible quantities are solved using some exemplary values for the parameters involved. This is followed by a specific treatment of transient Nd:YAG (where YAG is yttrium aluminum garnet) laser wave mixing in silicon and liquid crystals where some experimentally observed effects are well described by our present theory.

II. THEORY

The starting point of our analysis is the set of Maxwell equations governing the propagation of the lasers within the nonlinear medium

$$\nabla\times\mathbf{E}=\frac{1}{c}\frac{\partial\mathbf{H}}{\partial t} \tag{1}$$

and

$$\nabla\times\mathbf{H}=\frac{1}{c}\frac{\partial\mathbf{D}}{\partial t} \ . \tag{2}$$

The displacement vector $\mathbf{D}$ is related to the optical electric field $\mathbf{E}$ via the constitutive equation

$$\mathbf{D}=(\epsilon+\Delta\epsilon)\mathbf{E} \ , \tag{3}$$

where ϵ is the linear optical dielectric constant and $\Delta\epsilon$ is the optically induced change in the dielectric constant. We are using notation very similar to that used in Refs. 5 and 10 for the purpose of comparison. Consider the interaction geometry as depicted in Fig. 1. The two incident waves are labeled 1 (strong pump beam) and -1 (weak probe beam), respectively. In general, there are several diffracted beams on the transmitted side, and they are labeled ± 3, ± 5, and so on. We will be concerned with wave mixing involving beams and cross sections much larger than the thickness of the film, and therefore we can safely use the plane-wave approximation. In this case, the field variables depend only on x and z, i.e., the Maxwell equation for a charge- and current-free medium becomes

$$\frac{\partial^2 E}{\partial x^2}+\frac{\partial^2 E}{\partial z^2}-\frac{\epsilon}{c^2}\frac{\partial^2 E}{\partial t^2}=\frac{1}{c^2}\frac{\partial^2(\Delta\epsilon E)}{\partial t^2} \ . \tag{4}$$

Because of the oscillatory behavior of $\Delta\epsilon$ in the x direction generated by the interference of the two coherent input beams 1 and -1, we may expand the field and the dielectric constant in terms of their Fourier components, i.e., we have

$$E=E_y(x,z,t)=\sum_m E_m(z,t)e^{i(\omega t-k_z z+mk_x x)} \ , \tag{5}$$

$$\Delta\epsilon=\Delta\epsilon(x,z,t)=\sum_l \epsilon_l(z,t)e^{ilk_x x} \ , \tag{6}$$

where $m=\pm 1,\pm 3,\ldots$. For simplicity, we have assumed that all the fields are linearly polarized in the y direction.

Substituting Eqs. (5) and (6) into Eq. (4) yields

$$-i\frac{\epsilon}{2k_z c^2}\frac{\partial^2 E_m}{\partial t^2}+\frac{i}{2k_z}\frac{\partial^2 E_m}{\partial t^2}+\frac{\epsilon\omega}{c^2 k_z}\frac{\partial E_m}{\partial t}+\frac{\partial E_m}{\partial z}$$
$$+i(1-m^2)\frac{k_x^2}{2k_z}E_m+\frac{\alpha}{2}E_m=-i\frac{k_0^2}{2k_z}\sum_l \epsilon_l E_{m-l} \ . \tag{7}$$

The last term $(\alpha/2)E_m$ on the left-hand side is a phenomenological loss term that we add on to account for losses (e.g., scattering, absorption, etc.) in the nonlinear medium experienced by all the optical fields.

Assuming the slowly varying envelope approximations, all the second-derivative terms are small in comparison with the first derivative, and Eq. (7) becomes simply

$$\frac{\partial E_m}{\partial z}-iK_m E_m+\frac{\alpha}{2}E_m=-iK_0\sum_l \epsilon_l E_{m-l} \ , \tag{8}$$

where

$$K_0=\frac{k_0^2}{2k_z}=\frac{\pi}{\lambda_0[n^2-\sin^2(\theta/2)]^{1/2}} \tag{9}$$

and

$$K_m=(m^2-1)\frac{k_x^2}{2k_z} \ . \tag{10}$$

The wave-mixing processes, whether it is two wave, three wave, or multiwave, depend, to a large extent, on the functional form of $\Delta\epsilon$ on the optical field and spatial and temporal coordinates. The functional form of $\Delta\epsilon$, of course, is dictated by the physical mechanisms (e.g., thermal, electronic, orientational, photorefractive, etc.) and also the various time scales involved (decay time, turn-on time, and laser pulse lengths).

In this paper, we consider a class of nonlinear mechanism where the optical dielectric constant change obeys an equation of the form

$$\frac{\partial(\Delta\epsilon)}{\partial t}=\beta E^2-\frac{\Delta\epsilon}{\tau_0}+D_x\frac{\partial^2\Delta\epsilon}{\partial x^2}+D_z\frac{\partial^2\Delta\epsilon}{\partial z^2} \ . \tag{11}$$

The first term on the right-hand side describes the optically induced dielectric constant change per unit time. The second term is the relaxation of the dielectric constant by nondiffusive mechanisms (e.g., recombination of

carriers, radiative relaxations from excited levels, etc.). The last two terms describe the diffusive relaxation processes.

This equation describes many electronic, thermal, orientational, and other diffusive nonlinear processes (e.g., such as the electronic valence → conduction transition nonlinearity studied by Eichler *et al.*, and the thermal and orientational nonlinearities in liquid crystal).[6,12] In the latter cases, the z dependence of $\Delta\epsilon$ may also be represented by a sine function [e.g., the z dependence of the laser-induced thermal refractive index change in a nematic-liquid-crystal film is of the form $\sin(\pi z/d)$]. Using $\epsilon_l(z,t)=\epsilon_l(t)\sin(\pi z/d)$ in (6), and substituting (6) into (11) above yield an equation for the lth Fourier component of $\Delta\epsilon$

$$\frac{\partial(\Delta\epsilon)_l}{\partial t}=(\beta E^2)_l-\frac{(\Delta\epsilon)_l}{\tau_l} \tag{11'}$$

where

$$\tau_l^{-1}=D_x k_x^2 l^2+D_z\frac{\pi^2}{d^2} . \tag{12}$$

The reorientation effect in liquid crystals is described by a similar equation with the replacement of D by the appropriate elastic constant.[13,14] In liquid crystals' thermal and reorientational effects, τ_0 is not involved.

To explicitly describe the roles played by the phases and phase shifts among the beams and between the intensity and index gratings we shall express the complex field amplitude E_n by a real amplitude $\sqrt{I_n}$ and a phase ϕ_n, i.e.,

$$E_n=\sqrt{I_n}e^{i\phi_n} . \tag{13}$$

Equation (12) can first be integrated to give

$$\epsilon_l=-\beta\int_0^t\sum_n\sqrt{I_nI_{n-l}}\exp\left[i\phi_{n,l}(t')-\frac{(t-t')}{\tau_l}\right]dt' , \tag{14}$$

where $l=\pm2,\pm4,\pm6$ since $n=\pm1,\pm3$.

Also

$$\phi_{i,j}\equiv\phi_i-\phi_{i-j} . \tag{15}$$

Substituting Eqs. (13) and (14) into (8), we get the equation for the amplitude $\sqrt{I_m}$ and the phase ϕ_m of the coupled optical fields

$$\frac{\partial\sqrt{I_m}}{\partial z}=-\frac{\alpha}{2}\sqrt{I_m}-\beta k_0\sum_l\sqrt{I_{m-l}}\int_0^t\sum_n\sqrt{I_nI_{n-l}}\exp\left[\frac{t'-t}{\tau_l}\right]\sin[\phi_{n,l}(t')-\phi_{m,l}(t)]dt , \tag{16}$$

$$\frac{\partial\phi_m}{\partial z}=k_m+\frac{\beta k_0}{\sqrt{I_m}}\sum_l\sqrt{I_{m-l}}\int_0^t\sum_n\sqrt{I_nI_{n-l}}\exp\left[\frac{t'-t}{\tau_l}\right]\cos[\phi_{n,l}(t')-\phi_{m,l}(t)]dt . \tag{17}$$

Equations (16) and (17) above are similar to those in Ref. 10, where only a perturbative solution is given. The perturbative solution assumes that the gain experienced by the probe beam, $\Delta I_{-1}/I_{-1}$ is small compared to unity. Also, the diffracted beams are not accounted for.

On the other hand, in Ref. 5, one of the diffracted beams (I_3) is included in the calculation. However, the three-beam picture used is only valid for a probe beam (I_1) that is very weak compared to the pump beam; this three-beam model, as we remarked earlier, will not be able to describe the wave mixing dependence on the pump to probe beam intensity ratio β (c.f. Refs. 4 and 6 on stationary multiwave mixing effects).

To quantitatively describe recently observed experimental results (Refs. 4 and 5), and to predict the dependences of the probe gain on all the parameters involved, it is imperative, as is done here, that at least four beams be included in the formalisms.

Writing out Eqs. (16) and (17) explicitly for $m=\pm1,\pm3$, we get

$$\begin{aligned}\frac{\partial\sqrt{I_1}}{\partial z}=&-\frac{\alpha}{2}\sqrt{I_1}-\beta k_0\left[\sqrt{I_{-1}}\int_0^t e^{(t'-t)/\tau_2}\{\sqrt{I_1I_{-1}}\sin[\phi_{1,2}(t')-\phi_{1,2}(t)]+\sqrt{I_{-1}I_{-3}}\sin[\phi_{-1,2}(t')-\phi_{1,2}(t)]\right.\\&\left.+\sqrt{I_3I_1}\sin[\phi_{3,2}(t')-\phi_{1,2}(t)]\}dt'\right.\\&+\sqrt{I_3}\int_0^t e^{(t'-t)/\tau_2}\{\sqrt{I_1I_3}\sin[\phi_{1,-2}(t')-\phi_{1,-2}(t)]\\&+\sqrt{I_{-1}I_1}\sin[\phi_{-1,-2}(t')-\phi_{-1,-2}(t)]\\&+\sqrt{I_{-3}I_{-1}}\sin[\phi_{-3,-2}(t')-\phi_{1,-2}(t)]\}dt'\\&+\sqrt{I_{-3}}\int_0^t e^{(t'-t)/\tau_4}\{\sqrt{I_1I_{-3}}\sin[\phi_{1,4}(t')-\phi_{1,4}(t)]\\&\left.+\sqrt{I_3I_{-1}}\sin[\phi_{3,4}(t')-\phi_{1,4}(t)]\}dt'\right] ,\end{aligned} \tag{18}$$

$$\frac{\partial\sqrt{I_{-1}}}{\partial z}=-\frac{\alpha}{2}\sqrt{I_{-1}}-\beta k_0\left[\sqrt{I_1}\int_0^t e^{(t'-t)/\tau_2}\{\sqrt{I_1I_3}\sin[\phi_{1,-2}(t')-\phi_{-1,-2}(t)]+\sqrt{I_{-1}I_1}\sin[\phi_{-1,-2}(t')-\phi_{-1,-2}(t)]+\sqrt{I_{-3}I_{-1}}\sin[\phi_{-3,-2}(t')-\phi_{-1,-2}(t)]\}dt'+\sqrt{I_{-3}}\int_0^t e^{(t'-t)/\tau_2}\{\sqrt{I_1I_{-1}}\sin[\phi_{1,2}(t')-\phi_{-1,2}(t)]+\sqrt{I_{-1}I_{-3}}\sin[\phi_{-1,2}(t')-\phi_{-1,2}(t)]+\sqrt{I_3I_1}\sin[\phi_{3,2}(t')-\phi_{-1,2}(t)]\}dt'+\sqrt{I_3}\int_0^t e^{(t'-t)/\tau_4}\{\sqrt{I_{-1}I_3}\sin[\phi_{-1,-4}(t')-\phi_{-1,-4}(t)]+\sqrt{I_{-3}I_1}\sin[\phi_{-3,-4}(t')-\phi_{-1,-4}(t)]\}dt'\right], \tag{19}$$

$$\frac{\partial\sqrt{I_{-3}}}{\partial z}=-\frac{\alpha}{2}\sqrt{I_{-3}}-\beta k_0\left[\sqrt{I_{-1}}\int_0^t e^{(t'-t)/\tau_2}\{\sqrt{I_1I_3}\sin[\phi_{1,-2}(t')-\phi_{-3,-2}(t)]+\sqrt{I_{-1}I_1}\sin[\phi_{-1,-2}(t')-\phi_{-3,-2}(t)]+\sqrt{I_{-3}I_{-1}}\sin[\phi_{-3,-2}(t')-\phi_{-3,-2}(t)]\}dt'+\sqrt{I_1}\int_0^t e^{(t'-t)/\tau_4}\{\sqrt{I_{-1}I_3}\sin[\phi_{-1,-4}(t')-\phi_{-3,-4}(t)]+\sqrt{I_{-3}I_1}\sin[\phi_{-3,-4}(t')-\phi_{-3,-4}(t)]\}dt'+\sqrt{I_3}\int_0^t e^{(t'-t)/\tau_6}\{\sqrt{I_{-3}I_3}\sin[\phi_{-3,-6}(t')-\phi_{-3,-6}(t)]\}dt'\right], \tag{20}$$

$$\frac{\partial\sqrt{I_3}}{\partial z}=-\frac{\alpha}{2}\sqrt{I_3}-\beta k_0\left[\sqrt{I_1}\int_0^t e^{(t'-t)/\tau_2}\{\sqrt{I_1I_{-1}}\sin[\phi_{1,2}(t')-\phi_{3,2}(t)]+\sqrt{I_{-1}I_{-3}}\sin[\phi_{-1,2}(t')-\phi_{3,2}(t)]+\sqrt{I_3I_1}\sin[\phi_{3,2}(t')-\phi_{3,2}(t)]\}dt'+\sqrt{I_{-1}}\int_0^t e^{(t'-t)/\tau_4}\{\sqrt{I_1I_{-3}}\sin[\phi_{1,4}(t')-\phi_{3,4}(t)]+\sqrt{I_3I_{-1}}\sin[\phi_{3,4}(t')-\phi_{3,4}(t)]\}dt'+\sqrt{I_{-3}}\int_0^t e^{(t'-t)/\tau_6}\sqrt{I_3I_{-3}}\sin[\phi_{3,6}(t')-\phi_{3,6}(t)]dt'\right], \tag{21}$$

$$\frac{\partial\phi_1}{\partial z}=\beta k_0\left[\tau I_0e^{-\alpha z}(1-e^{-t/\tau})+\left[\frac{I_{-1}}{I_1}\right]^{1/2}\int_0^t e^{(t'-t)/\tau_2}\{\sqrt{I_1I_{-1}}\cos[\phi_{1,2}(t')-\phi_{1,2}(t)]+\sqrt{I_{-1}I_{-3}}\cos[\phi_{-1,2}(t')-\phi_{1,2}(t)]+\sqrt{I_{-3}I_{-1}}\cos[\phi_{-3,-2}(t')-\phi_{1,-2}(t)]\}dt'+\left[\frac{I_3}{I_1}\right]^{1/2}\int_0^t e^{(t'-t)/\tau_4}\{\sqrt{I_1I_3}\cos[\phi_{1,-2}(t')-\phi_{1,-2}(t)]+\sqrt{I_{-1}I_1}\cos[\phi_{-1,-2}(t')-\phi_{1,-2}(t)]+\sqrt{I_{-3}I_{-1}}\cos[\phi_{-3,-2}(t')-\phi_{1,-2}(t)]\}dt'+\left[\frac{I_{-3}}{I_1}\right]^{1/2}\int_0^t e^{(t'-t)/\tau_4}\{\sqrt{I_1I_3}\cos[\phi_{1,-3}(t')-\phi_{1,4}(t)]+\sqrt{I_3I_{-1}}\cos[\phi_{3,4}(t')-\phi_{1,4}(t)]\}dt\right], \tag{22}$$

$$\frac{\partial\phi_2}{\partial z}=\beta k_0\left[\tau I_0 e^{-\alpha z}(1-e^{-t/\tau})\right.$$
$$+\left(\frac{I_1}{I_{-1}}\right)^{1/2}\int_0^t e^{(t'-t)/\tau_2}\{\sqrt{I_1 I_3}\cos[\phi_{1,-2}(t')-\phi_{-1,2}(t)]$$
$$+\sqrt{I_{-1}I_1}\cos[\phi_{-1,-2}(t')-\phi_{-1,-2}(t)]$$
$$+\sqrt{I_{-3}I_{-1}}\cos[\phi_{-3,-2}(t')-\phi_{-1,-2}(t)]\}dt'$$
$$+\left(\frac{I_{-3}}{I_{-1}}\right)^{1/2}\int_0^t e^{(t'-t)/\tau_2}\{\sqrt{I_1 I_{-1}}\cos[\phi_{1,2}(t')-\phi_{-1,2}(t)]$$
$$+\sqrt{I_{-1}I_{-3}}\cos[\phi_{-1,2}(t')-\phi_{-1,2}(t)]$$
$$+\sqrt{I_3 I_1}\cos[\phi_{3,2}(t')-\phi_{-1,2}(t')]\}dt'$$
$$+\left(\frac{I_3}{I_{-1}}\right)^{1/2}\int_0^t e^{(t'-t)/\tau_4}\{\sqrt{I_{-1}I_3}\cos[\phi_{-1,-4}(t')-\phi_{-1,-4}(t)]$$
$$\left.+\sqrt{I_{-3}I_1}\cos[\phi_{-3,-4}(t')-\phi_{-1,-4}(t)]\}dt'\right], \tag{23}$$

$$\frac{\partial\phi_3}{\partial z}=k_3+\beta k_0\left[\tau_0 I_0 e^{-\alpha z}(1-e^{-t/\tau})\right.$$
$$+\left(\frac{I_1}{I_3}\right)^{1/2}\int_0^t e^{(t'-t)/\tau_2}\{\sqrt{I_1 I_{-1}}\cos[\phi_{1,2}(t')-\phi_{3,2}(t)]$$
$$+\sqrt{I_{-1}I_{-3}}\cos[\phi_{-1,2}(t')-\phi_{3,2}(t)]$$
$$+\sqrt{I_3 I_1}\cos[\phi_{3,2}(t')-\phi_{3,2}(t)]\}dt'$$
$$+\left(\frac{I_{-1}}{I_3}\right)^{1/2}\int_0^t e^{(t'-t)/\tau_4}\{\sqrt{I_1 I_{-3}}\cos[\phi_{1,4}(t')-\phi_{3,4}(t)]$$
$$+\sqrt{I_3 I_{-1}}\cos[\phi_{3,4}(t')-\phi_{3,4}(t)]\}dt'$$
$$\left.+\left(\frac{I_{-3}}{I_3}\right)^{1/2}\int_0^t e^{(t'-t)/\tau_6}\{\sqrt{I_3 I_{-3}}\cos[\phi_{3,6}(t')-\phi_{3,6}(t)]\}dt'\right], \tag{24}$$

$$\frac{\partial\phi_{-3}}{\partial z}=k_{-3}+\beta k_0\left[\tau I_0 e^{-\alpha z}(1-e^{-t/\tau})\right.$$
$$+\left(\frac{I_{-1}}{I_{-3}}\right)^{1/2}\int_0^t e^{(t'-t)/\tau_2}\{\sqrt{I_1 I_3}\cos[\phi_{1,-2}(t')-\phi_{-3,-2}(t)]$$
$$+\sqrt{I_{-1}I_1}\cos[\phi_{-1,-2}(t')-\phi_{-3,2}(t)]$$
$$+\sqrt{I_{-3}I_{-1}}\cos[\phi_{-3,-2}(t')-\phi_{-3,-2}(t)]\}dt'$$
$$+\left(\frac{I_1}{I_{-3}}\right)^{1/2}\int_0^t e^{(t'-t)/\tau_4}\{\sqrt{I_{-1}I_3}\cos[\phi_{-1,-4}(t')-\phi_{-3,-4}(t)]$$
$$+\sqrt{I_{-3}I_1}\cos[\phi_{-3,-4}(t')-\phi_{-3,-4}(t)]\}dt'$$
$$\left.+\left(\frac{I_3}{I_{-3}}\right)^{1/2}\int_0^t e^{(t'-t)/\tau_6}\{\sqrt{I_{-3}I_3}\cos[\phi_{-3,-6}(t')-\phi_{-3,-6}(t)]\}dt'\right]. \tag{25}$$

Notice that there are three gratings, and therefore three-grating decay time constants τ_2, τ_4, and τ_6 involved. This is very different from the two-wave mixing model considered by Vinetskii *et al.*, and the two-wave and three-wave models by Eichler *et al.*, where only one grating and therefore one decay time constant τ_2 is used.

III. GENERAL DISCUSSION

Equations (18)–(22) show explicitly the coupling of the four laser-beam intensities and phases. They reflect both *transient two-wave mixing* (TTWM) *terms* and *transient multiwave mixing* (TMWM) terms. If we focus our attention on the right-hand side of the equation for the probe-beam intensity I_{-1}, for example, these terms can be clearly identified. The TTWM terms involve only the probe beam (I_{-1}) and one other beam (e.g., terms containing $\sqrt{I_1}\sqrt{I_{-1}I_1}$, or $\sqrt{I_{-3}}\sqrt{I_{-1}I_{-3}}$, $\sqrt{I_3}\sqrt{I_3I_1}$, etc.). On the other hand, the TMWM terms involve at least two other beams besides the probe beam (e.g., $\sqrt{I_1}\sqrt{I_1I_3}$, $\sqrt{I_1}\sqrt{I_{-3}I_{-1}}$, $\sqrt{I_3}\sqrt{I_{-3}I_1}$, etc.).

For the purpose of the present discussion, we will denote a typical TTWM term by T_2. From the first line of the right-hand side of Eq. (19) an example of T_2 is

$$T_2(I)=\sqrt{I_1}\int_0^t e^{(t'-t)/\tau_2}\sqrt{I_{-1}I_1}\times\sin\{[\phi_{-1}(t')-\phi_1(t')]-[\phi_{-1}(t)-\phi_1(t)]\}dt' . \tag{26}$$

On the other hand, transient multiwave mixing terms may be denoted as $T_{m's}$. An example is

$$T_m(I)=\sqrt{I_1}\int_0^t e^{(t'-t)/\tau_2}\sqrt{I_1I_3}\times\sin\{[\phi_1(t')-\phi_3(t')]-[\phi_{-1}(t)-\phi(t)]\}dt' . \tag{27}$$

Similar terms may be identified in the phase equations. The terms corresponding to (26) and (27) above are, respectively,

$$T_2(I)=\left[\frac{I_1}{I_{-1}}\right]^{1/2}\int_0^t e^{(t'-t)/\tau_2}\sqrt{I_{-1}I_1}\times\cos\{[\phi_{-1}(t')-\phi_1(t')]-[\phi_{-1}(t)-\phi_1(t)]\}dt' , \tag{28}$$

$$T_m(\phi)=\left[\frac{I_1}{I_{-1}}\right]^{1/2}\int_0^t e^{(t'-t)/\tau_2}\sqrt{I_1I_3}\times\cos\{[\phi_1(t')-\phi_3(t')]-[\phi_{-1}(t)-\phi_1(t)]\}dt' . \tag{29}$$

It is obvious that the contribution from these transient two-wave and multiwave mixing terms to the generation and/or growth of the beams involved depend, to a large extent, on the phases and phase shifts, and the intensities of all the beams (incident and diffracted). They in turn depend on the initial conditions.

To study the dynamics of these processes, we will consider step-function input lasers, i.e.,

$$I_{10,-10}(t)=\begin{cases}0, & t<0\\ I_{10,-10}, & t>0\end{cases} . \tag{30}$$

The initial conditions for the amplitude of the beams are therefore

$$\sqrt{I_1}=\sqrt{I_{10}} , \tag{31}$$

$$\sqrt{I_{-1}}=\sqrt{I_{-10}} , \tag{32}$$

$$\sqrt{I_3}=0=\sqrt{I_{-3}} . \tag{33}$$

From Eqs. (18)–(25), and these initial conditions, we get, at $z=0$,

$$[\phi_3(t,0)-\phi_1(t,0)]+[\phi_{-1}(t',0)-\phi_1(t',0)]=\frac{\pi}{2} , \tag{34}$$

$$[\phi_{-3}(t,0)-\phi_{-1}(t,0)]+[\phi_{-1}(t',0)-\phi_1(t',0)]=\frac{\pi}{2} , \tag{35}$$

for all t'.

If the two incident beams are coherent, $\phi_1(t',0)-\phi_1(t',0)=\text{const}=\phi_{-1}(0,0)-\phi_1(0,0)$, which we can conveniently set equal to zero. We therefore have

$$\phi_{-1}(0,0)=\phi_1(0,0)=0 , \tag{36}$$

$$\phi_3(t,0)=-\phi_1(t,0)=\pi/2 , \tag{37}$$

$$\phi_{-3}(t,0)=-\phi_1(t,0)=\pi/2 . \tag{38}$$

From Eqs. (18)–(25), we can also prove that

$$\frac{\partial I}{\partial z}=-\alpha I , \tag{39}$$

where $I=I_1+I_{-1}+I_3+I_{-3}$, i.e.,

$$I_0=I|_{z=0}=I_{10}+I_{-10} , \tag{40}$$

where I_0 is the total input intensity at $z=0$.

These explicit classifications of intensity and phase in accordance with their two-wave or many-wave transient mixing effects are important for comparison between the transient case under consideration here and the stationary case considered in previous studies. In the stationary case, i.e., $t\gg\tau$, all the phases will be stationary (i.e., $\partial\phi/\partial t=0$). An examination of all the *two-wave mixing terms* show that in this regime, they contribute negligibly to the variation in intensities because of the *sine factor* [c.f., Eq. (26) for $T_2(I)$], although they still contribute to variations in the phase because of the *cosine factor* [c.f. Eq. (28) for $T_2(\phi)$]. On the other hand, because the multiwave mixing effect involves more than two beams at a time, and therefore two different phase shifts [c.f. Eq. (27) for $T_m(I)$ and Eq. (29) for $T_m(\phi)$] in general, their contributions to the intensity and phase variations persist even for a large time.

Because of the presence of both two-wave and multiwave mixing effects, and the strong coupling of all the phases, in general, there will be strong interference effects between these processes. These interference effects will be strongly governed by the presence or absence of the diffracted beams, which in turn depend largely on the phase mismatches $K_{\pm 3}d$, where d is the interaction length.

IV. NUMERICAL RESULTS

In this section, we present the solutions of Eqs. (18)–(25) for some experimentally accessible quantities, using some exemplary set of values for the interaction length d, the intensities, wave mixing angles, etc. From the previous discussions on Eqs. (18)–(25) for the coupled wave equations, Eq. (11) for $\Delta\epsilon$, and Eq. (12) for τ, we note that these multiwave mixing processes depend on a few fundamental quantities which are identified as follows. If we concern ourselves with diffusive types of nonlinearities, i.e., ignore τ_0 in Eq. (12), then the fundamental unit of time is τ_2. From Eq. (12) for $\Delta\epsilon$, we note that another fundamental parameter is the quantity $\tau_2\beta I_0$, which gives a measure of the dielectric constant charge induced by the total intensity. Apart from these two parameters, the other obvious parameters are the wave mixing angle θ [which affects τ_2 through k_x^2 dependence on θ in Eq. (11)], the interaction length d, and the absorption constant α. Equations (18)–(25) are solved by temporal integration in units of t/τ_6, since τ_6 is the shortest time scale. The choice of values for $\tau_2\beta I_0$ is governed by experimental data in studies where transient wave mixing induced probe gain has been observed. Typically, $\tau_2\beta I_0$ should be on the order of 10^{-3} or 10^{-4} (i.e., the refractive index change has to be on this order), for $d \approx 0.1$–0.5 mm or so, for a sizeable probe gain to occur. We will return to this more experimental oriented discussion in Sec. V. Using these typical "practical" values for τ_6, β, d, I_0, etc., the solution of the coupled equations (18)–(25) yield several new interesting observations.

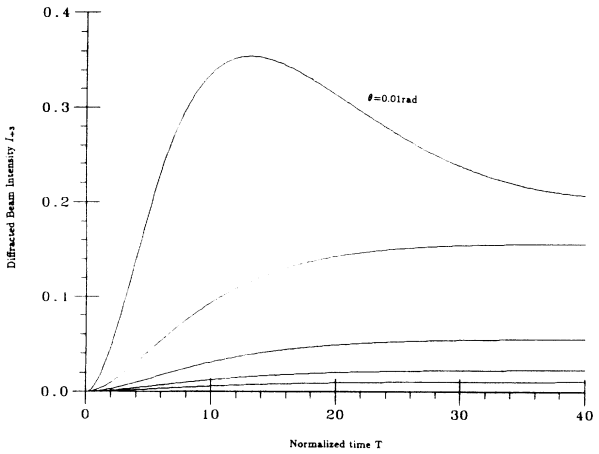

FIG. 3. Dependence of the diffracted beam I_3 as a function of the normalized time $T=t/\tau_6(\theta)$ for $\theta=0.01$ (uppermost curve), 0.015, 0.02, 0.025, and 0.03 rad (lowest curve) for the same parameters as in Fig. 2.

Figure 2 shows plots of the normalized time ($T=t/\tau_6$) dependence of transmitted probe-beam intensity $I_{-1}(d)$ for several values of the wave mixing angles θ. [Note that τ_2, τ_4, and τ_6 are all functions of the wave mixing angle, c.f. Eq. (12)]. The general trends of the probe-beam intensity as a function of the normalized time (t/τ_6) are similar to those of the diffracted beams I_3 and I_{-3} shown in Figs. 3 and 4, respectively. For $\theta=0.01$, there is an initial "bump" followed by a gradual approach to a steady-state value of 12.5 (not shown in Fig. 2, but can be seen in Fig. 5). The *highest gain* [defined as

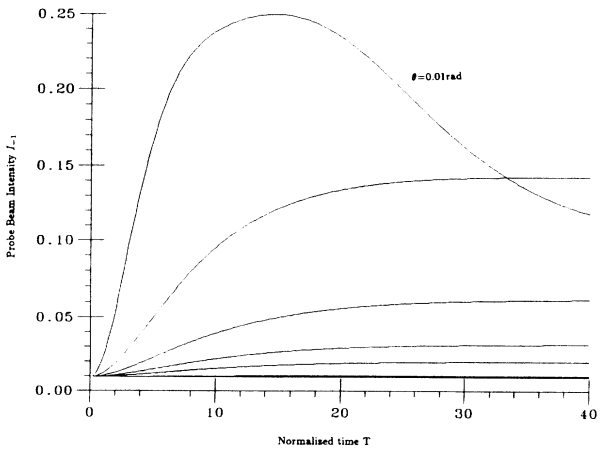

FIG. 2. Dependence of the transmitted probe beam as a function of the normalized time $T=t/\tau_6(\theta)$ for various wave mixing angles in radians ($\theta=0.01, 0.015, 0.02, 0.025, 0.03, 0.05, 0.07$). The uppermost curve corresponds to $\theta=0.01$. The other parameter used is $\beta I=10^{-3}$ sec^{-1}, $I_{-1}(0)/I_1(0)=0.01$, $d=0.5$ mm, $\alpha=1$ cm^{-1}. As a reference, τ_6 for $\theta=0.01$ is 3×10^{-8} sec.

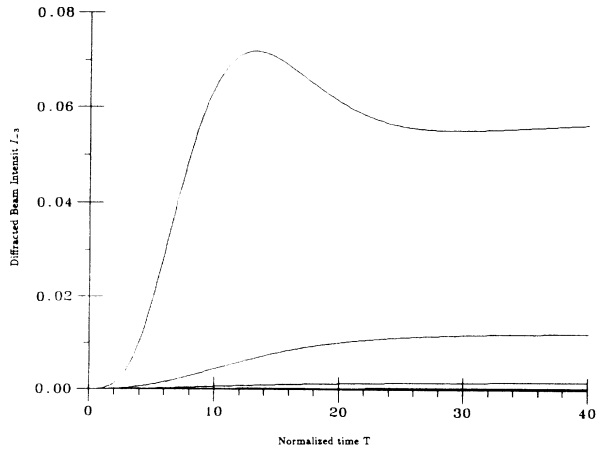

FIG. 4. Dependence of the diffracted beam I_{-3} as a function of the normalized time $T=t/\tau_6(\theta)$. There are nonzero contributions only for $\theta=0.01$ (uppermost curve), 0.015, 0.02, and 0.025 rad (lowest curve), for the same parameters used in Fig. 2.

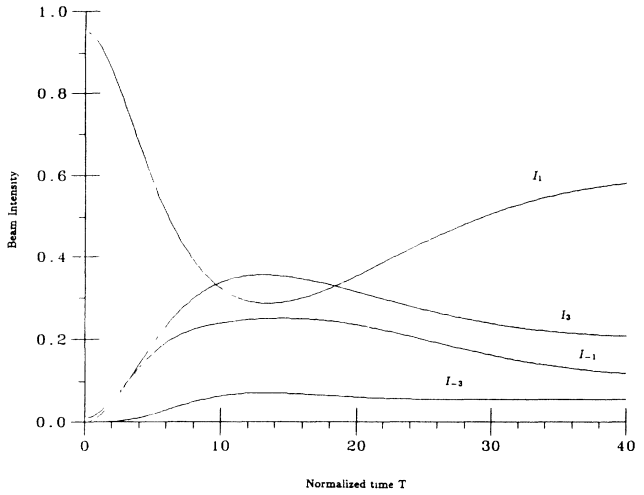

FIG. 5. Plot of the intensities of all the four beams involved in the wave mixing process as a function of the normalized time $T=t/\tau_6$ for $\theta=0.01$; other parameters are the same as in Fig. 2.

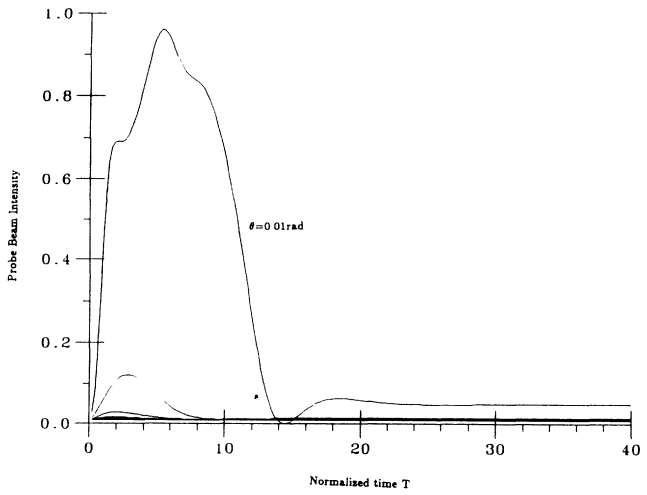

FIG. 6. Plot of the probe beam as a function of the normalized time $T=t/\tau_2$ for $\theta=0.01$ (highest peak curve), $\theta=0.015$, 0.02, and 0.025, considering only two-wave (I_{-1} and I_1) mixing. Other parameters are the same as in Fig. 2.

$I_{-1}(d)/I_{-1(0)}$] achievable (at the peak of the bump) is about 25. For larger angles, the intensity rises monotonically to a steady-state value (with a gain of about 14). As the wave mixing angle θ increases, these gains decrease rapidly. At $\theta=0.07$, there is essentially no gain (Fig. 2). From the $\theta=0.05$ curves in Figs. 2 and 3, and comparing with the curves of higher θ values in these two figures, we can see that there is no steady-state gain in I_{-1} if I_3 is of diminishing value. This is expected from our previous analysis of stationary multiwave mixing effect, where the amplification of the probe beam I_{-1} requires the presence of I_3 (in conjunction with the pump beam I_1). From Fig. 5, which plots all these four beams as a function of time for the case $\theta=0.01$, one can see that the probe beam I_{-1} and the two diffracted beams I_3 and I_{-3} all reach the highest values at about the same instant ($t/\tau_6\approx 11$), where the pump beam actually drops to a value below I_3 and is comparable to I_{-1}.

The seemingly smooth rise of the intensity of I_{-1}, as depicted in Fig. 2, and the time coincidence of the peaks of I_{-1} and I_3 should not be interpreted to mean that the probe-beam gain is largely due to four-wave mixing effect alone (i.e., the scattering of I_1 from the grating formed by I_1 and I_3 into the I_{-1} direction). Rather, as we will presently see, the results for I_{-1} and all other beams in Figs. 2–5 are the end product of very strongly coupled multiwave mixing effects [following Eqs. (18)–(25)] involving strong phase shifts and interference effects among the beams.

These strong interference effects may be seen if one considers only the *two-wave mixing* terms in Eqs. (18)–(15), i.e., interaction involving only I_1 and I_{-1}. Using the same set of parameters used in obtaining Fig. 2, the intensities of the probe beam I_{-1} due to two-wave mixing with I_1 are plotted as a function of time for $\theta=0.01,0.015,0.025,0.03$, etc. as shown in Fig. 6. For $\theta=0.01$, one notes that the intensity of I_{-1} reaches a value as high as 0.95 at $t/\tau_6=5$, which means I_1 is almost entirely depleted. On the other hand, the multiwave mixing picture (c.f. Fig. 5) gives a I_{-1} of about 0.2 at $t/\tau_6=5$, and a maximum at $t/\tau_6=11$. At $t/\tau_6=11$, the value of I_{-1} is actually almost vanishing in the two-wave mixing picture (c.f. Fig. 6). By these comparisons, one can deduce that (i) strong interference effects occur owing to the multiwave mixing effect to "smooth out" the gain of I_{-1}, leading to a maximum value much lower than if only I_{-1} and I_1 are involved; and (ii) generation of I_{-3} and I_3 of substantial magnitude (c.f. Fig. 5, where for $\theta=0.01$, I_3 can be larger than I_{-1}) also lowers the gain of I_{-1}. The interference effects also arise from the large variation in the relative phases among the beams, which may be seen in Figs. 7 and 8, which show the

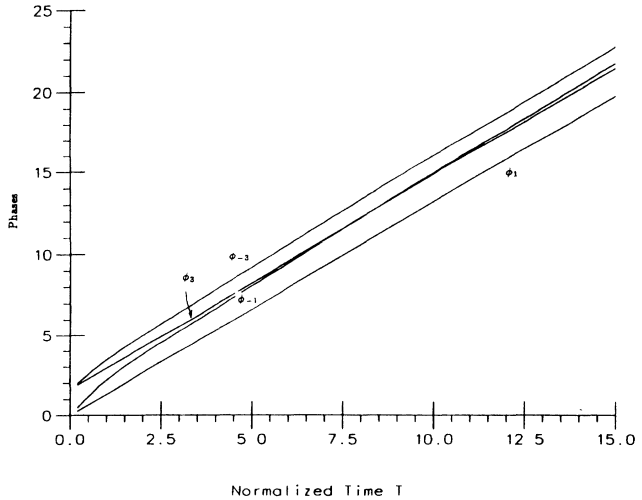

FIG. 7. Plot of the phases ϕ_1, ϕ_{-1}, ϕ_3, and ϕ_{-3} involved in the multiwave mixing process (c.f. Fig. 5), for $\theta=0.01$ rad as a function of the normalized time $T=t/\tau_6$.

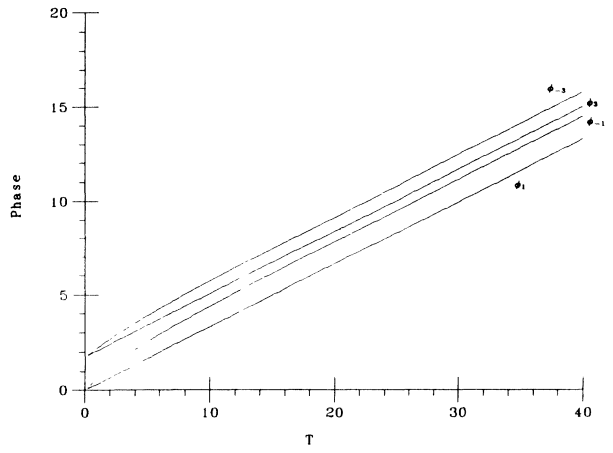

FIG. 8. Plot of the phases ϕ_1, ϕ_{-1}, ϕ_3, and ϕ_{-3} for the case $\theta=0.02$ as a function of the normalized time $T=t/\tau_6$.

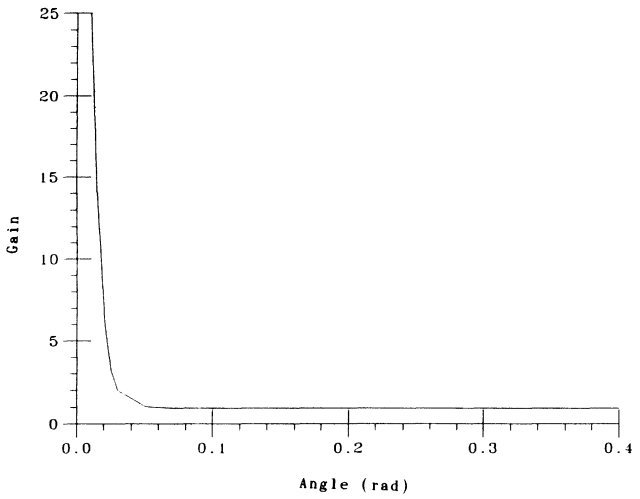

FIG. 9. Dependence of the maximal multiwave mixing mediated probe-beam gain on the wave mixing angle (in radians).

time-dependent phases ϕ_1, ϕ_{-1}, ϕ_3, and ϕ_{-3} for $\phi=0.02$, respectively. Starting from $\phi_1=\phi_{-1}=0$, one notes that at $t/\tau_6=10$, $\phi_{-1}-\phi_1\approx 70°$ (Fig. 7, for $\theta=0.01$).

A common feature of Figs. 2–4, and 6 is the drastic drop in the multiwave mixing effects (gain, diffraction, etc.) as a function of the wave mixing angle. This is exemplified by Fig. 9, which plots the gain of I_{-1} as a function of angle θ. The gain drops from a high of about 25 at $\theta=0.01$ to unity (i.e., no gain) at $\theta=0.03$. *There are two distinct reasons for this dependence on* θ. One is the more obvious phase-mismatch factor K_3 involved in the four-wave and multiwave mixing effect. The phase mismatch in distance d is given by $K_3 d\approx k\theta^2 d$. Using $\lambda=1.06$ μm, $d=0.5$ mm, $k_3 d\approx 0.1\pi$ for $\theta=0.01$ and $k_3 d\approx\pi$ for $\theta=0.03$. Clearly, the diffracted beams will be quenched for $\theta>0.03$, contributing therefore negligibly to the gain of I_{-1}.

The drop in the two-wave mixing gain (plotted in Fig. 10) is basically due to the diffusive nature of the nonlinear process [c.f. Eq. (11)] and the consequent dependence of the relaxation time τ on the wave mixing angle $\tau_l^{-1}\alpha D_x k_x^2 l^2 = D_x l^2 K^2 \sin^2(\theta/2)$ [ignoring the $D_x(\pi^2/d^2)$, as we have done throughout all the numerical calculations], i.e., $\tau_l \sim \sin^{-2}(\theta/2)$. Consider now the two-wave mixing term in the I_{-1} Eq. (19), we have

$$\frac{\partial\sqrt{I_{-1}}}{\partial_z}\sim\beta k_0 I_1\int_0^t e^{(t'-t)/\tau_2}\sqrt{I_{-1}}\times\sin\{[\phi_{-1}(t')-\phi_1(t')]-[\phi_{-1}(t)-\phi_1(t)]\}dt' . \quad (41)$$

In our numerical calculation, we use the normalized time $T=t/\tau_2$ (there is no τ_6 in two-wave mixing), Eq. (41) above becomes

$$\frac{\partial\sqrt{I_{-1}}}{\partial_z}\sim k_0\beta I_1\tau\int_0^t e^{(t'-t)/\tau_2}\sqrt{I_{-1}}\times\sin\{[\phi_{-1}(T')-\phi_1(T')]-[\phi_{-1}(T)-\phi_1(T)]\}dt' . \quad (42)$$

The corresponding equations for ϕ_1 and ϕ_{-1} are

$$\frac{\partial\phi_1}{\partial z}=\beta k_0\tau I_0 e^{-\alpha z}(1-e^{-T})+\beta k_0\tau\left[\frac{I_{-1}}{I_1}\right]^{1/2}\int_0^t e^{T'-T}\sqrt{I_{-1}I_1}\cos\{[\phi_{-1}(T')-\phi_1(T')]-[\phi_{-1}(T)-\phi_1(T)]\}dt' , \quad (43)$$

$$\frac{\partial\phi_{-1}}{\partial z}=\beta k_0\tau I_0 e^{-\alpha z}(1-e^{-T})+\beta k_0\tau\left[\frac{I_1}{I_{-1}}\right]^{1/2}\int_0^t e^{T'-T}\sqrt{I_{-1}I_1}\cos\{[\phi_{-1}(T')-\phi_1(T')]-[\phi_{-1}(T)-\phi_1(T)]\}dt' . \quad (44)$$

The magnitude of $\sqrt{I_{-1}}$ and ϕ's are very sensitively dependent on the coefficient $\beta\tau I_0$ appearing in these integrals, i.e., $I_{-1}(z)$ is very sensitively dependent on $\beta^2\tau^2 I_0^2$. Since τ drops off rapidly with increasing θ, the gain in the intensity of the transmitted I_{-1} also decreases rapidly with increasing value of θ for a fixed input intensity I_0. In Ref. 10, an approximate solution of Eqs. (41)–(44) above are given, valid for small gain $\Delta I_{-1}/I_{-1}<1$. The approximate perturbative solution shows that $\Delta I_{-1}/I_{-1}$ is proportional to $(\beta\tau I_0)^2$, similar to what we deduced above. Obviously a quantitative evaluation of I's and ϕ's must also take into account the variation of ϕ and I inside the integral and their subsequent effect on the integral itself. This can only be done numerically, as we have in getting the result plotted in Figs. 2–4, 6, 9, and 10. The results confirm our observa-

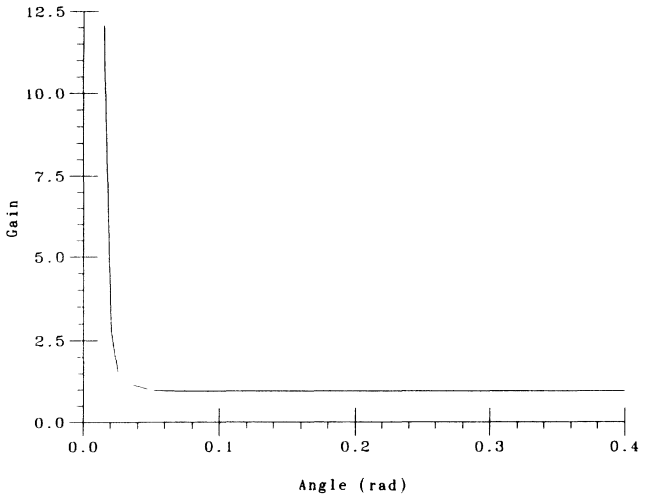

FIG. 10. Dependence of the maximal probe-beam gain in transient two-wave mixing on the wave mixing angle.

tion that the two-wave mixing effect is very sensitive to τ, or more appropriately $\tau\beta I_0$, and the wave mxing angles, as are the four-wave and multiwave mixing effects.

V. FURTHER REMARKS AND COMMENTS ON EXPERIMENTS

There have been numerous experimental studies of transient wave mixing effects in various materials in the past. Observations of large gain in thin nonlinear media where diffractions are present are made only recently.[4,5,15] The motivation for carrying out the preceding analysis lies in our need for a quantitative theory that includes effects due to these participating diffracted beams, and that allows one to see explicitly the role played by various parameters such as laser intensities, intensity ratio, wave mixing angle, thickness, nonlinear coefficient, and the various time scales. Using the preceding theory, one can quantitatively analyze the recently observed effects in semiconductor and liquid crystals, which, respectively, involve a laser of a widely varying time scale (picosecond and millisecond) and relaxation dynamics. In the case of the silicon experiment[5] by Eichler *et al.*, the observation of large wave mixing gain even at a relatively large angle (θ up to 18°) is simply due to the increased intensity of the picosecond laser used [$I_1(0)$ is 100 mJ/cm^2 in 50 ps] and the matching of the short laser pulse to the grating diffusion time constant of large angles.

The increased input pump beam intensity and its short duration have two important effects. One is the realization of a large optically induced dielectric constant change in a time (laser pulse width) comparable to the grating diffusion time. The other is the accompanying large (intensity-dependent) phase modulation effect which dominates over the phase mismatch (which depends on the wave mixing angle) experienced by the diffracted beam, as we will presently discuss.

In the experiment by Eichler *et al.*, the value of $\beta=(-2n\bar{\alpha}N_{e-h}/h\nu)$ is -0.373 cm^{2}J^{-1}, for N_{e-h} $\sim 10^{-21}$ cm^3, and $\bar{\alpha}=10$ cm^{-1}, and $h\nu=1.88\times10^{-19}$ J at $\lambda=1.06$ μm. For a wave mixing angle of 10°, for example, τ_6 is on the order of 79 ps (τ_2 of 700 ps). This gives a value for $\tau_6\beta I$ of 5.5×10^{-2}, which, in accordance with our preceding analysis, will produce large probe beam amplification effects. Such effects were reported by Eichler *et al.*[5(a)] and our recent study.[15]

At other angles of wave mixing, the associated grating diffusion time contants are matched to a better or lesser degree with the laser pulse duration, contributing to the angular variation in the observed gain. Using the experimental parameters mentioned above, and other experimental parameters [$d=0.4$ mm, $I_1(0)/I_{-1}(0)=100$, $\bar{\alpha}=10$ cm^{-1}, an intensity-dependent beam loss $\alpha=19$ cm^{-1} deduced from Ref. 5(b)], we are able to obtain a theoretical fit of the experimental curve [Fig. 1 of Ref. 5(a)] for the angular dependence of the probe gain[15] (cf. Fig. 11). It is important to note that even for large angles ($>3°$ where the phase mismatch k_3d is greater than π), where the side diffraction is usually thought to be quenched, the diffractions (especially I_3) nevertheless actually play a substantial role in providing gain to the probe beam via the multiwave mixing effect. This may be seen in the plot [cf. Figs. 12(a) and 12(b)] of the z dependence of I_3 for the same set of parameters used in getting Fig. 11, for θ ranging from 4.01° to 13.90°. As a result of both phase mismatches [from k_3 on the right-hand side of (24)] and comparable or even larger phase modulation effects [other terms on the right-hand side (24)], the diffraction can be of substantial magnitude within the nonlinear medium. This, together with the increased matching of the laser pulse with the grating diffusion time constant, all contribute to large probe-beam gain effect even at large angles. For these angles, if one had used purely two-wave mixing picture (i.e., throw away

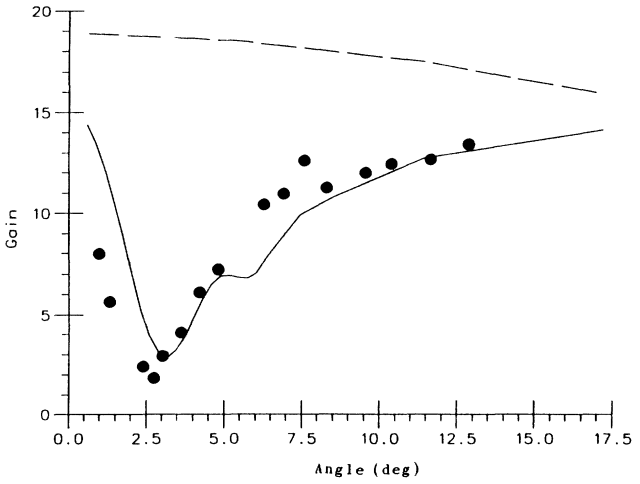

FIG. 11. Theoretical curve for the dependence of the probe-beam gain on the wave mixing angle in the transient wave mixing experiment by Eichler *et al.* (Ref. 5) on silicon with picosecond laser. Dots are experimental points deduced from Fig. 1 of Ref. 5. Long-dashed line is the theoretical curve obtained using a two-wave mixing model.

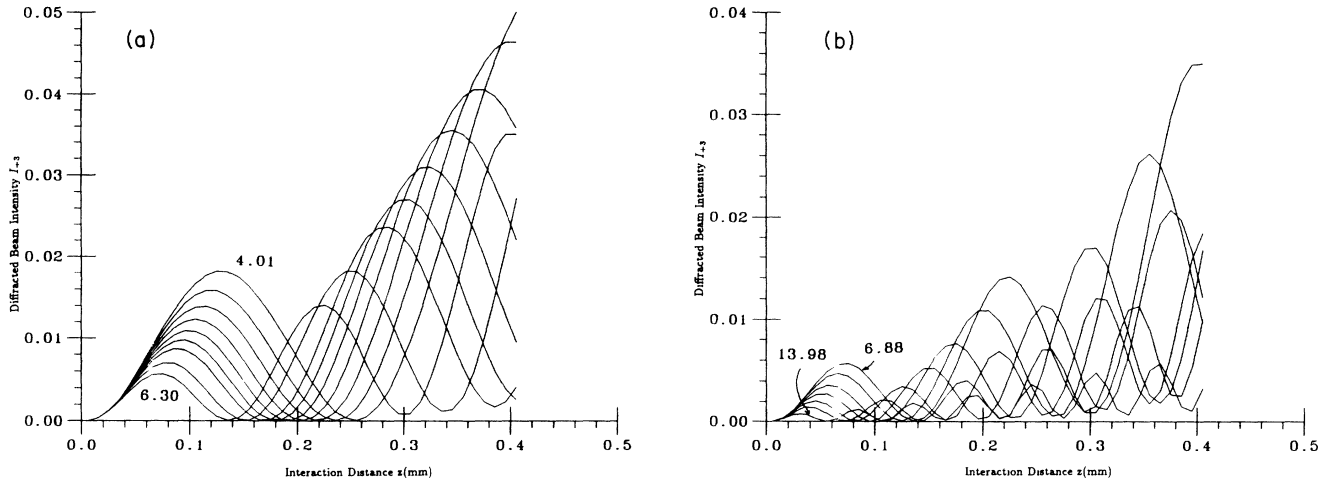

FIG. 12. Calculated dependence of the magnitude of the diffracted beam intensity I_3 on the interaction distance z, using the same set of experimental parameters as Fig. 11, for various wave mixing angles: (a) 4.01, 4.30°, 4.58°, 4.87°, 5.16°, 5.44°, 5.73°, 6.02°, 6.30°; (b) 6.88°, 7.45°, 8.31°, 9.17°, 10.31°, 11.46°, 13.98°. Note that the magnitude of the diffracted beam inside the nonlinear medium could reach a value far greater than the value at the exit plane (at $z=0.4$ mm) as a result of phase modulations and energy transfer among the beams.

I_3, I_{-3}), the theoretical results will deviate (in magnitude and form of dependence) far from the experimental observations (c.f. Fig. 11, dotted line). A multiwave picture, accounting for not only these diffractions, but also the inevitable phase shifts and modulation effects, is a necessity.

Using the parameters pertinent to liquid crystals, we can also explain recently observed large probe-beam amplification effects involving millisecond CO_2 laser pulses and the thermal nonlinearity. In the experiments[6] performed by Khoo *et al.*, and similarly by Sanchez, Kayour, and Huignard, the beam ratio used is about 100:1. The *total* change in dielectric constant $\Delta\epsilon$ induced by the laser near the phase-transition temperature T_c (for $T-T_c \approx 40°$ to $T=T_c$) estimated to be on the order of $\Delta\epsilon = 2n\Delta n \sim 2\times 1.5\times 0.05 = 0.15$. The dielectric constant grating amplitude $\Delta\epsilon_l$ is therefore on the order of $\Delta\epsilon_l \sim (1/100)\Delta\epsilon \sim 1.5\times 10^{-3}$, i.e., $\tau_6 \beta I \approx 10^{-3}$. Although this value for $\tau_6\beta I$ is smaller than in the silicon experiment, the smaller crossing angle used and the relatively longer pulse (40 ms compared to the grating decay time $\tau_6 = 3$ ms) may explain why an equally large probe amplification effect (gain ≈ 20) was observed. Detailed measurement of these amplification effects in liquid crystals using CO_2 laser pulses are currently underway and a quantitative comparison between the theory and experiments will be presented in a future publication.

ACKNOWLEDGMENTS

This research is supported by the National Science Foundation, Grant No. ECS 8712078.

[1]S. A. Akhmanov, A. P. Sikhorukov, and R. V. Khokhlov, Usp. Fiz. Nauk **93**, 19 (1967) [Sov. Phys.—Usp. **10**, 609 (1968)].

[2]R. Y. Chiao, P. L. Kelly, and E. Garmire, Phys. Rev. Lett. **17**, 1158 (1966); R. Y. Chiao, E. Garmire, and C. Townes, *ibid.* **13**, 479 (1964).

[3]See, for example, R.. Reintjes, *Nonlinear Optical Parametric Processes in Liquids aand Gases* (Academic, New York, 1983); see also, Y. R. Shen, *Principles of Nonlinear Optics* (Wiley, New York, 1984).

[4]I. C. Khoo and T. H. Liu, Phys. Rev. A **39**, 4036 (1989), and references therein; T. H. Liu and I. C. Khoo, IEEE J. Quantum Electron. **JQE23**, 2020 (1987); P. Y. Yan and I. C. Khoo, *ibid.* **JQE25**, 520 (1989).

[5](a) H. Eichler, M. Glotz, A. Kummrow, K. Richter, and X. Yang, Phys. Rev. A **35**, 4673 (1987); (b) I. C. Khoo and R. Normandin, Appl. Phys. Lett. **52**, 525 (1988).

[6]F. Sanchez, P. H. Kayour, and J. P. Huignard, J. Appl. Phys. **64**, 26 (1988); I. C. Khoo, P. Y. Yan, G. M. Finn, T. H. Liu, and R. R. Michael, J. Opt. Soc. Am. B **5**, 202 (1988), where, in the last section of the paper, the experimental results for probe-beam amplification with laser *pulses* are presented.

[7]L. Richard, J. Maurin, and J. P. Huignard, Opt. Commun. **57**, 365 (1986).

[8]I. C. Khoo and Y. Zhao, IEEE J. Quantum Electron. **JQE25**, 368 (1989).

[9]See, for example, *Photorefractive Materials and Their Applications,* edited by P. Gunter and J. P. Huignard (Springer-Verlag, Berlin 1988).

[10]V. L. Vinetskii, N. V. Kukhtarev, S. G. Odulov, and M. S. Soskin, Usp. Fiz. Nauk **129**, 113 (1979) [Sov. Phys.—Usp. **22(9)**, 742 (1979)].

[11]For *two-wave* mixing mediated ring oscillator, see, for exam-

ple, Pochi Yeh, J. Opt. Soc. Am. B **2**, 1924 (1985); D. Z. Anderson and R. Saxena, *ibid.* **4**, 164 (1987); G. Pauliat, M. Ingold, and P. Gunter, IEEE J. Quantum Electron. **25**, 201 (1989).

[12]H. Hsiung, L. P. Shi, and Y. R. Shen, Phys. Rev. A **30**, 1453 (1984).

[13]I. C. Khoo, in *Progress in Optics,* edited by E. Wolf (North-Holland, Amsterdam, 1988), Vol. XXVI.

[14]I. C. Khoo, R. R. Michael, and P. Y. Yan, IEEE J. Quantum Electron. **QE23**, 267 (1987).

[15]I. C. Khoo, P. Zhou, R. G. Lindquist, and P. LoPresti, Phys. Rev. A **41**, 408 (1990).